

This is a repository copy of *Subtle Microwave-Induced Overheating Effects in an Industrial Demethylation Reaction and Their Direct Use in the Development of an Innovative Microwave Reactor*.

White Rose Research Online URL for this paper:

<https://eprints.whiterose.ac.uk/id/eprint/115748/>

Version: Accepted Version

Article:

De Bruyn, Mario orcid.org/0000-0002-9687-1606, Budarin, Vitaliy L., Sturm, Guido S.J. et al. (4 more authors) (2017) Subtle Microwave-Induced Overheating Effects in an Industrial Demethylation Reaction and Their Direct Use in the Development of an Innovative Microwave Reactor. *Journal of the American Chemical Society*. pp. 5431-5436. ISSN: 1520-5126

<https://doi.org/10.1021/jacs.7b00689>

Reuse

Items deposited in White Rose Research Online are protected by copyright, with all rights reserved unless indicated otherwise. They may be downloaded and/or printed for private study, or other acts as permitted by national copyright laws. The publisher or other rights holders may allow further reproduction and re-use of the full text version. This is indicated by the licence information on the White Rose Research Online record for the item.

Takedown

If you consider content in White Rose Research Online to be in breach of UK law, please notify us by emailing eprints@whiterose.ac.uk including the URL of the record and the reason for the withdrawal request.

Subtle Microwave-Induced Overheating Effects in an Industrial Demethylation Reaction and Their Direct Use in the Development of an Innovative Microwave Reactor

Mario De bruyn,[†] Vitaliy L. Budarin,[†] Guido S. J. Sturm,^{||} Georgios D. Stefanidis,[‡] Marilena Radoiu,[§] Andrzej Stankiewicz,^{||} and Duncan J. Macquarrie^{*,†}

[†]Green Chemistry Centre of Excellence, University of York, YO10 5DD, Heslington, York, United Kingdom

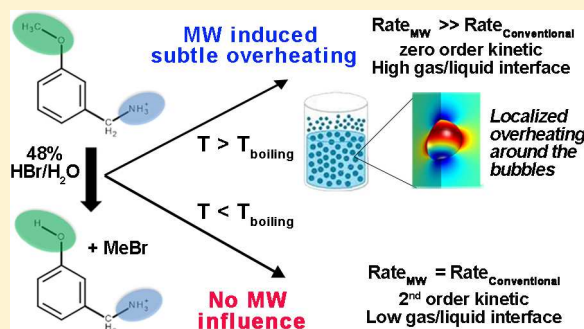
[‡]Catholic University of Leuven (KU Leuven), Process Engineering for Sustainable Systems Section, Willem de Croylaan 46-box 2423, 3001 Leuven, Belgium

[§]SAIREM, 12 Porte du Grand Lyon, 01702 NEYRON Cedex, France

^{||}Process & Energy Department, Delft University of Technology, Leeghwaterstraat 39, 2628CB Delft, The Netherlands

S Supporting Information

ABSTRACT: A systematic study of the conventional and microwave (MW) kinetics of an industrially relevant demethylation reaction is presented. In using industrially relevant reaction conditions the dominant influence of the solvent on the MW energy dissipation is avoided. Below the boiling point, the effect of MWs on the activation energy E_a and k_0 is found nonexistent. Interestingly, under reflux conditions, the microwave-heated (MWH) reaction displays very pronounced zero-order kinetics, displaying a much higher reaction rate than observed for the conventionally thermal-heated (CTH) reaction. This is related to a different gas product (methyl bromide, MeBr) removal mechanism, changing from classic nucleation into gaseous bubbles to a facilitated removal through escaping gases/vapors. Additionally, the use of MWs compensates better for the strong heat losses in this reaction, associated with the boiling of HBr/water and the loss of MeBr, than under CTH. Through modeling, MWH was shown to occur inhomogeneously around gas/liquid interfaces, resulting in localized overheating in the very near vicinity of the bubbles, overall increasing the average heating rate in the bubble vicinity vis-à-vis the bulk of the liquid. Based on these observations and findings, a novel continuous reactor concept is proposed in which the escaping MeBr and the generated HBr/water vapors are the main driving forces for circulation. This reactor concept is generic in that it offers a viable and low cost option for the use of very strong acids and the managed removal/quenching of gaseous byproducts.



INTRODUCTION

The 20th century has been mainly dominated by the use of conventional thermal energy to drive chemical reactions. The use of alternative energy sources, such as microwave (MW) technology, appeared in the late 1970s, and its use could overcome existing bottlenecks in chemical manufacturing and improve the carbon footprint of many reactions.¹ While it is clear that poor instrumentation has led to erroneous reports and set off unrealistic expectations,² a systematic and controlled investigation of the influence of MWs on chemical reactions and their kinetics has been lacking. Such background information is however indispensable for possible future implementation of MW technology on an industrial scale. To date, many types of thermal and nonthermal MW effects have been reported; as a guide to past research in these reports, the interested reader is referred to the critical review by De La Hoz and co-workers.³ Presently, many of the “nonthermal MW effects” have been disproven as being the result of an incorrect

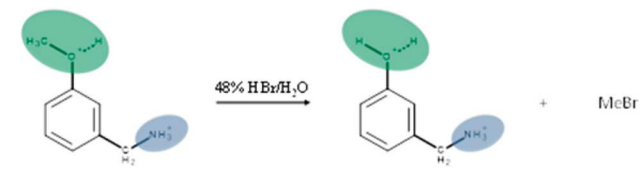
temperature measurement. Also, the energy contained in MWs is far too low to break even hydrogen bonds.⁴ In the presence though of non-MW absorbing solvents the groups of Dudley and Stiegman argue that both substrate and product can temporarily store energy, leading to localized temperature increases at the reactive site, accounting for the observed MW rate enhancements.⁵ More recently they also showed that poorly MW-absorbing molecules can be selectively heated by MWs provided association to a nonreactive polar molecule as a good MW absorber, albeit the effect is then less pronounced.⁶ In a further advancement the Kappe group used Si–C vessels which were proclaimed to impede the penetration of MWs into the reaction vessel, heating the Si–C material instead, and thus administering in essence conventional heating. That way no difference in reactivity could be observed between conventional

Received: January 26, 2017

Published: March 27, 2017

64 and MW heated reactions.⁷ However, very recently the Strouse
 65 group showed convincingly that 3 mm Si–C tube walls only
 66 retain ~48% of the MWs, pointing at significant MW
 67 transmission into, and dissipation inside, the reaction vessel.
 68 This MW leakage through Si–C tube walls is particularly
 69 acute when a strongly absorbing solvent is used.⁸ Fan et al. have
 70 pioneered the use of MW technology to the hydrothermal
 71 depolymerization of cellulose to glucose, demonstrating a
 72 distinct influence of the applied MW density and a MW heat
 73 input via molecular radiators;⁹ notably, they used proton/
 74 deuterium exchange techniques to also obtain structural
 75 information. Many research groups continue to propose
 76 differing activation energies for reactions run in the presence
 77 of CTH vis-à-vis MWH. However, the determination of the
 78 kinetic parameters (E_a , k_0) of a reaction strongly depends on
 79 the applied model and thus requires a solid understanding of
 80 the reaction mechanism. Also, a sufficient number of data
 81 points is needed to ensure confidence, thus requiring a
 82 thorough analytical method. In this study we have investigated
 83 the MW activation of an industrially (pharmaceutically)
 84 relevant demethylation reaction, converting (3-
 85 methoxyphenyl)methylammonium bromide (3MPMA) into
 86 (3-hydroxyphenyl)methylammonium bromide (3HPMA) (see
 87 Scheme 1)^{10,11} with a detailed kinetics study. For this purpose,

Scheme 1. Overview of the Reaction



88 we have used both a SAIREM MiniFlow200SS¹² with TM
 89 monomode cavity and an Anton Paar Monowave 300, both of
 90 which are equipped with fiber-optic temperature measurement.
 91 The MiniFlow200 uses a solid-state MW generator, which
 92 enables precise frequency and microwave power control; in
 93 addition, it features forward and reflected power measurement
 94 so that an energy balance can be obtained. The absence of this
 95 latter feature in most commonly used MW heating equipment
 96 has been demonstrated to result in significant misreadings of
 97 the actual MW power transferred to the sample under
 98 investigation.¹³ The experimental study is complemented by a
 99 simulation study to obtain additional insight into the interacting
 100 physical phenomena: electromagnetics, fluid dynamics, and
 101 heat transfer. The demethylation reaction in this study is
 102 typically run on multitonne scale and generally employs limited
 103 amounts of solvent and reagents, therewith increasing the
 104 efficiency of the process and its productivity. This reaction
 105 however has received little mechanistic attention, especially
 106 under relevant reaction conditions. From a MW point of view,
 107 the investigation of a polar reaction with high substrate/
 108 product dipoles and continuously changing dielectric proper-
 109 ties, as the reaction progresses, presents a great opportunity to
 110 gain more knowledge and understanding of how the use of
 111 MWs could potentially benefit such chemical reactions.¹⁴

112 ■ DISCUSSION

113 To assess the potential influence of different heating methods
 114 on the 3MPMA to 3HPMA demethylation reaction, kinetic
 115 reaction profiles (as conversion–time plots) were first

established for the case of an open vessel CTH covering the
 90–118 °C temperature range (Figure 1A). The reaction

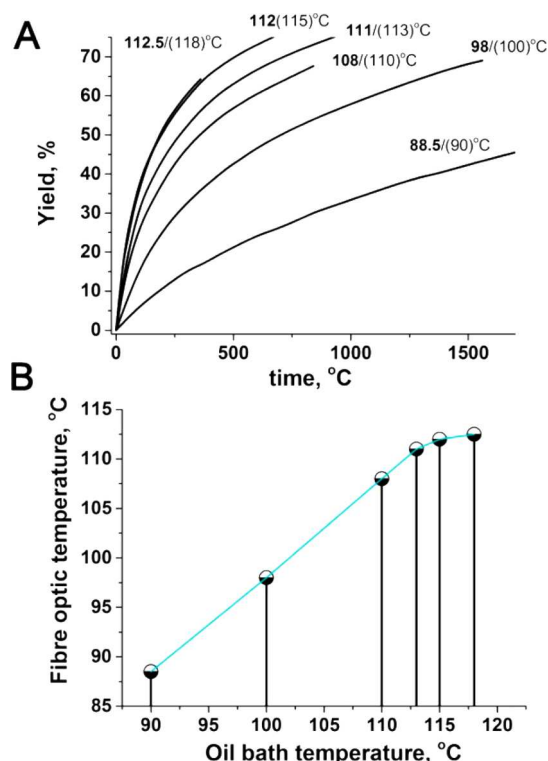


Figure 1. (A) Conversion–time plots for the CTH reaction. The temperatures displayed in bold are measured by internal fiber-optic probe while those in brackets refer to oil bath temperatures. (B) Comparison between the target (oil bath) temperatures and the temperatures recorded by internal fiber-optic probe.

mixture consisted of 5.038 g of 3MPMA (0.0367 mol) and 12.38 g of 48% HBr (0.0734 mol HBr; twice excess vis-à-vis substrate), and no additional solvent was added. Temperature measurement was performed in a dual way, recording both the oil bath temperature and, by fiber-optic temperature probe (FOTP), the internal reaction temperature. Interestingly, Figure 1A shows that the rate of the reaction becomes equal for oil bath temperatures ≥ 115 °C, equating by FOTP to an effective internal maximal reaction temperature of 112–112.5 °C. A linear correlation between the target (oil bath) temperatures and the recorded fiber-optic temperatures is observed only up to 113 °C (oil bath) (Figure 1B).

Kinetic analysis of the reaction profiles in Figure 1A shows a complex kinetic behavior which can generally not be explained as a single first- or second-order process for the entire conversion range. More specifically, the beginning and the end of the reaction appear to behave as different consecutive second-order processes, which interchange at the 50–60% conversion level (Figure 1S). In the 90 °C case, the conversion level is below 50% showing thus only the first process. To explain this complex behavior, it was hypothesized that throughout the reaction the number of available protons is reduced by (reversible) protonation of 3HPMA (Scheme 1S). This becomes particularly important in the later stages of the reaction, as close to stoichiometric amounts of reagents are employed in this reaction. As shown in Figure 2, this model (Scheme 1S, eq 15a) fits the experimental kinetic data very well for all temperatures. In a second approach, conversion–time

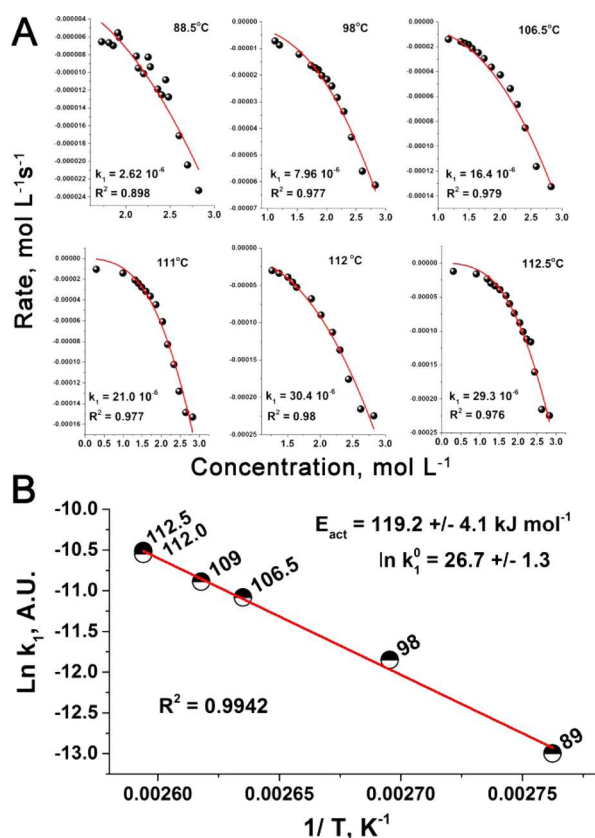


Figure 2. (A) Plots of the “reaction rate” to “substrate concentration” data for the CTH reaction and consequent fitting of the two-step model shown in Scheme 1S (eq 15a). (B) Calculated E_a and k_0 values for the CTH reaction displayed in Scheme 1S.

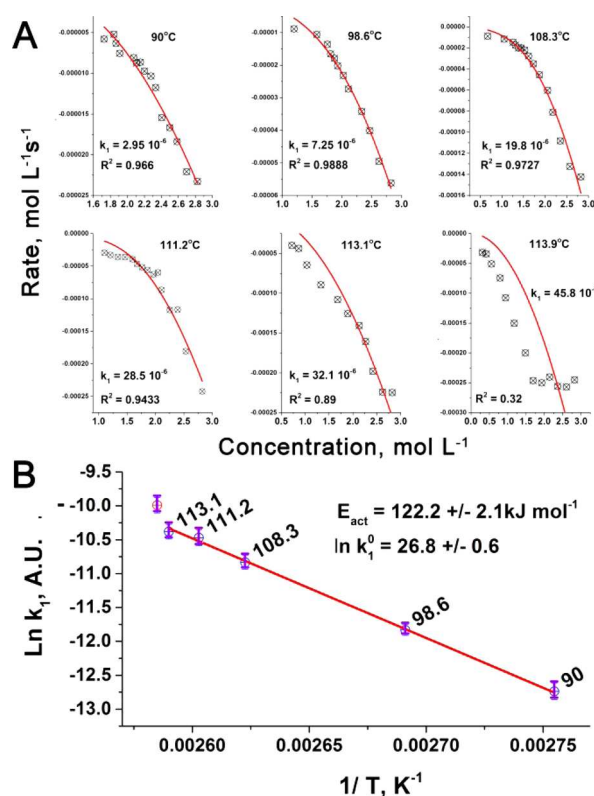


Figure 3. (A) Plots of the “reaction rate” to “substrate concentration” data for the MWH reaction and consequent fitting of the two-stage model (Scheme 1S). (B) Calculated E_a and k_0 values for the MWH reaction.

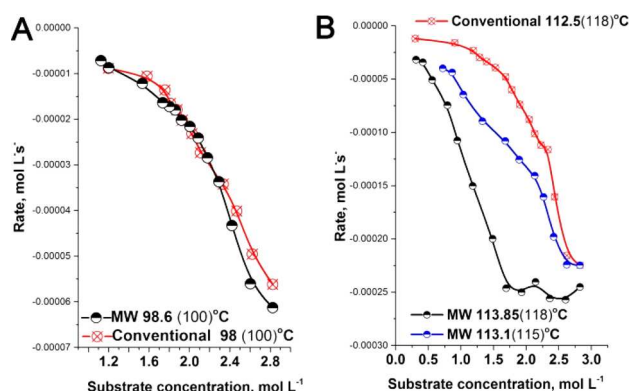


Figure 4. Illustrative overlays of the “reaction rate–substrate concentration” plots for the ConvTH and MWH reactions at 100 °C (A) and 118 °C (B).

heating of water in a MW field, including a laminar fluid dynamics model to simulate the free convection under nonstirring conditions.¹³ In addition, for the continuous flow case, Patil et al. presented an experimentally verified numerical study into a MW heated millireactor; in particular, they demonstrated temperature measurement deviations due to large thermal gradients around the sensor.¹⁶ To model the MWH demethylation reaction case adequately, a much more advanced methodology was required, covering all the relevant physical phenomena and stirring. Furthermore, to correctly predict the electromagnetic field inside the cavity and the reactor, knowledge was required of the dielectric properties of the reaction mixture at the relevant temperatures. The medium

properties were measured and determined to be $\epsilon' = 17$ and $\sigma = 3.3$ S/m. The dissipative (σ) term is best described as an electrical conductivity due to the high concentration of ions in solution. A visual set up is provided in Figure 5a, and additional

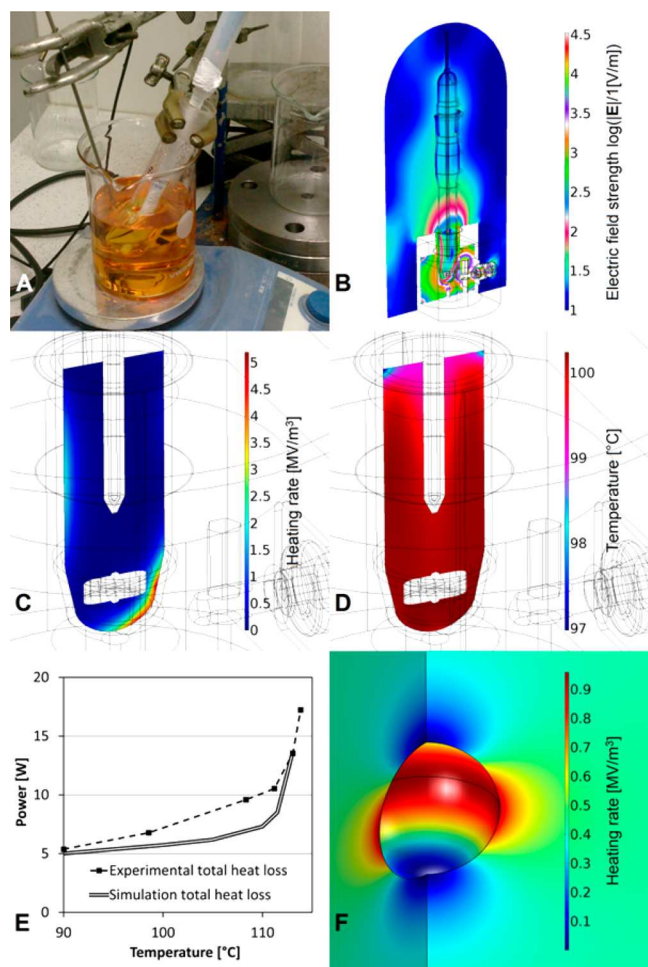


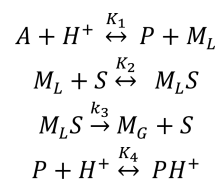
Figure 5. Simulation results of electromagnetic dissipation and heat transfer. (A) Visual setup for measurement of the dielectric properties. (B) MW field in and around the cavity applicator and reactor. (C) Heating rate distribution. (D) Temperature distribution in the reactor. (E) Overall electromagnetic dissipation in both the simulated and the experimental case versus temperature. (F) Heating rate around a bubble.

details are available from Supporting Information and Table 1S. The fluid agitation in the reactant mixture was simulated by applying a rotating geometrical domain, to account for stirrer bar rotation, in combination with the k - ϵ Reynolds-averaged Navier–Stokes model accounting for turbulence and turbulent heat transfer. Figure 5b–e shows the main modeling results for the multiphysics simulation. Additionally, an animated video is available from Supporting Information (video 1S). More specifically Figure 5b shows the MW field (by means of the electric field intensity on logarithmic scale) in and around the cavity applicator and reactor. The simulation shows that the electromagnetic emission and dissipation in the reactor and cavity construction materials are negligible. In addition, it also reconfirms the general nonuniformity of MW fields.¹³ The latter feature also expresses itself in the heat generation simulation presented in Figure 5c, where it can be seen that the main zone of heat generation occurs close to the MW antenna

of the cavity. However, in Figure 5d it is shown that for the applied stirring speed, the temperature variations in the reactor are too small to have any significant effect on the reaction rate, i.e., less than 1.5% rate variation for the highest temperatures and less than 0.4% below 111 °C. Figure 5e displays the overall electromagnetic dissipation and heat loss to the surroundings versus temperature for both the simulated and the experimental case. It can be seen that the simulation correctly approximates the characteristics of the experimental energy balance. The curves lie close to each other, and both have an accelerating heat loss as the temperature approaches the boiling point. Figure 5f shows a quasi-electrostatic analysis of the MW field around a bubble. The MW field is deformed by the presence of the bubble. Red zones, representing localized overheating, and blue zones, indicative of relatively cooler zones, can be observed. These however do not cancel out: there is a ~40% average increase in heat generation in a layer of ~0.1 times the bubble radius. Generally the evaporation of hydrobromic acid into a bubble extracts heat from the reactant liquid adjacent to this bubble due to the expansion of the bubble, which can result in a reduction of vapor pressure and consequently a potential bubble collapse. Though the flow regime in the reactor is turbulent due to stirring, the Kolmogorov length scale is calculated to be 30 to 240 μm .¹⁷ Below this scale, bubbles do not benefit from turbulent convective heat transfer, and their growth potential is limited unless a directly adjacent heat source is present. For the CTH case, only the bubbles contacting the heated reactor wall can grow, so that fewer and larger bubbles are formed. In comparison, for the MWH case, the presence of a locally enhanced volumetric heat source enables many more bubbles to form. This mechanism agrees well with the differences in boiling regime observed during experimentation; illustrative videos of the MWH (video 2S) and CTH (videos 3S and 4S) demethylation reaction at 112 °C are included in Supporting Information.

As the removal of MeBr gas through water/HBr vapor will be governed by the available surface between the reaction mixture and the water vapor bubbles, the occurrence of zero-order kinetics may relate to the available interface becoming insufficient to remove all produced MeBr formed at one given point in time. Scheme 2 represents the proposed

Scheme 2. Proposed Alternative Model for the Demethylation Reaction under MW Exposure at High Reaction Temperatures^a



^aA is 3MPMA, P is 3HPMA, M_L is methyl bromide in the liquid phase, M_G is methyl bromide in the gas phase, and S is the surface of the bubbles.

mechanism for higher temperature MW operation. The as-derived rate equation fits the high temperature MW kinetic data very well (see Scheme 2S, eq 28b, and Figure 2S). An additional observation in the MW transmission transient during experiments can be made; Figure 3S shows that fluctuations in the power regulation occur less rapidly with increasing reaction temperature, which indicates a change in medium properties as

the reactant mixture progresses from mechanism 1 to 2. Further to the use of open vessel reactors, we also evaluated the use of a closed vessel, i.e., using a pressure NMR tube for CTH and an Anton Paar MW closed vessel for the MWH reaction. As shown in Table 1, no distinct MW influence is observed when

Table 1. Conversion Levels for the Demethylation Reaction Performed at 118 °C in an Anton Paar MW Closed Vessel and, for the Conventional Heated Counterpart, an NMR Pressure Tube

entry	reactor type	conversion (%)		
		2 h reaction time	4 h reaction time	6 h reaction time
1	Anton Paar MW closed vessel reactor ^a	49.5	64.4	70.9
2	conventional by NMR pressure tube ^a	47.6	64.5	70.7

^aRatio gas to liquid phase in Anton Paar reaction vessel and NMR pressure tube are the same.

the reaction is performed in a closed vessel reactor. Indeed, in closed vessel operation no mass-transfer limitation problem arises as the produced MeBr builds up a pressure of ~110 psi (54.7% conversion) (Figure 4S), in that way shifting the equilibrium from MeBr gas to MeBr liquid.

The observation of intense steam/gas bubble production in the high temperature MWH reaction provided an interesting opportunity for the development of a novel continuous MW reactor concept in which MW energy is actually converted to kinetic energy, i.e., the escaping MeBr, and the generated HBr/water vapor can drive the reaction mixture around a loop. This concept is similar to gas/air-lift reactors, which find common application in industrial biotechnology and multiphase processes, but contrary to the concept proposed here, these rely on the introduction of a separate gas/air stream.¹⁸ The development of a continuous MW reactor for the demethylation reaction presented here holds distinct industrial advantages, notably (1) a controlled release and thus manageable scrubbing of toxic MeBr, (2) a continuous all-glass reactor concept tailored to the use of strongly corrosive acids, avoiding the need for expensive specialty alloys (e.g., Hastelloy), (3) the avoidance of an expensive pumping system capable of withstanding MeBr/HBr, (4) the absence of moving parts, and (5) enhanced mass transfer properties. Figures 5S and 6S show respectively the schematics of the circular and the continuous MW reactor. A video of the circular MW reactor in operation, employing a PI of 140 W, is included in Supporting Information (video 5S), and the conversion–time plots are shown in Figure 7S.

CONCLUSION

In summary, we have shown that the main influence of MWH, vis-à-vis CTH, on the kinetic parameters of an industrially relevant demethylation reaction occurs only under reflux conditions. Thus, the use of MWs opens a different mechanism for the elimination of gaseous byproducts (e.g., MeBr), by the creation of vast amounts of bubbles, therewith changing the observed reaction order of the demethylation reaction from 2 to 0. Through modeling, the origin of this change in reaction order was shown to relate to a deformation of the microwave field in the presence of bubbles, leading to localized overheating in the close vicinity of the bubbles. Based on these insights, a

novel continuous MW reactor concept could be proposed in which MW energy is converted into kinetic energy, making the production and removal of MeBr the driving force for the reactor. This offers a generic reactor concept for reaction types in which significant amounts of gaseous byproducts (e.g., de(m)ethylation, metathesis, dehydration) are created.

ASSOCIATED CONTENT

Supporting Information

, and illustrative videos are available in the Supporting Information. The Supporting Information is available free of charge on the ACS Publications website at DOI: 10.1021/jacs.7b00689.

Experimental details, additional figures, and reaction schemes/models (PDF)

Simulation results of SAIREM TM cavity for demethylation of (3-methoxyphenyl)methylammonium bromide (MPG)

Illustrative video of the MWH demethylation reaction at 112 °C (MPG)

Illustrative video of the CTH demethylation reaction at 112 °C (MPG)

Illustrative video of the CTH demethylation reaction at 112 °C (MPG)

Video of the circular MW reactor in operation employing a PI of 140 W (MPG)

AUTHOR INFORMATION

Corresponding Author

*E-mail: Duncan.Macquarrie@york.ac.uk.

ORCID

Duncan J. Macquarrie: 0000-0003-2017-7076

Notes

The authors declare no competing financial interest.

ACKNOWLEDGMENTS

The authors thank the European Research Council for the FPVII ALTEREGO project with grant number FP7-NMP-2012-309874. M.D.b. thanks Ms. A. Storey for the specialty glassware and Mr. C. Mortimer for consultation on practical reactor development. G.S.J.S. acknowledges Dr. J. W. R. Peeters for valuable feedback on the turbulence modeling, as well as the support staff of COMSOL B.V. (Zoetermeer, NL) for their prompt technical support.

REFERENCES

- (1) Wathey, B.; Tierney, J.; Lidstrom, P.; Westman, J. *Drug Discovery Today* **2002**, 7, 373–380.
- (2) Kappe, C. O.; Pieber, B.; Dallinger, D. *Angew. Chem., Int. Ed.* **2013**, 52, 1088–1094.
- (3) de la Hoz, A.; Diaz-Ortiz, A.; Moreno, A. *Chem. Soc. Rev.* **2005**, 34, 164–178.
- (4) Kappe, C. O. *Angew. Chem., Int. Ed.* **2013**, 52, 7924–7928.
- (5) Dudley, G. B.; Richert, R.; Stiegman, A. E. *Chem. Sci.* **2015**, 6, 2144–2152.
- (6) Wu, Y.; Gagnier, J.; Dudley, G. B.; Stiegman, A. E. *Chem. Commun.* **2016**, 52, 11281–11283.
- (7) Kappe, C. O. *Acc. Chem. Res.* **2013**, 46, 1579–1587.
- (8) Ashley, B.; Lovingood, D. D.; Chiu, Y.-C.; Gao, H.; Owens, J.; Strouse, G. F. *Phys. Chem. Chem. Phys.* **2015**, 17, 27317–27327.
- (9) Fan, J. J.; De Bruyn, M.; Budarin, V. L.; Gronnow, M. J.; Shuttleworth, P. S.; Breeden, S.; Macquarrie, D. J.; Clark, J. H. *J. Am. Chem. Soc.* **2013**, 135, 11728–11731.

- 362 (10) Breckenridge, R. J.; Nicholson, S. H.; Nicol, A. J.; Suckling, C. J.;
363 Leigh, B.; Iversen, L. *J. Neurochem.* **1981**, *37*, 837–844.
- 364 (11) Travnicek, Z.; Sipl, M.; Popa, I. *J. Coord. Chem.* **2005**, *58*, 1513–
365 1521.
- 366 (12) Christiaens, S.; Vantghem, X.; Radoiu, M.; Vanden Eynde, J. J.
367 *Molecules* **2014**, *19*, 9986–9998.
- 368 (13) Sturm, G. S. J.; Verweij, M. D.; van Gerven, T.; Stankiewicz, A.
369 I.; Stefanidis, G. D. *Int. J. Heat Mass Transfer* **2012**, *55*, 3800–3811.
- 370 (14) Waghmode, S. B.; Mahale, G.; Patil, V. P.; Renalson, K.; Singh,
371 D. *Synth. Commun.* **2013**, *43*, 3272–3280.
- 372 (15) Robinson, J.; Kingman, S.; Irvine, D.; Licence, P.; Smith, A.;
373 Dimitrakis, G.; Obermayer, D.; Kappe, C. O. *Phys. Chem. Chem. Phys.*
374 **2010**, *12*, 4750–4758.
- 375 (16) Patil, N. G.; Benaskar, F.; Meuldijk, J.; Hulshof, L. A.; Hessel,
376 V.; Schouten, J. C.; Esveld, E. D. C.; Rebrov, E. V. *AIChE J.* **2014**, *60*,
377 3824–3832.
- 378 (17) Pope, S. B. *Turbulent flows*; Cambridge University Press:
379 Cambridge, 2000.
- 380 (18) Drandev, S.; Penev, K. I.; Karamanev, D. *Chem. Eng. Sci.* **2016**,
381 *146*, 180–188.